Semiconductor Monolithic Wavelength Converter (SIPAS)

Yasuo Shibata[†], Yuichi Tohmori, Satoshi Oku, and Toshio Ito

Abstract

This paper describes the operating principle, structure, fabrication technology, and basic characteristics of a newly developed wavelength converter called a SIPAS. In a SIPAS, a Mach-Zehnder interferometer with a semiconductor optical amplifier in each arm is monolithically integrated with a Sagnac interferometer. Filter-free wavelength conversion with output pulse width of 13 ps due to differential-phase-modulation has been achieved using a fabricated SIPAS. The power penalty is as low as 0.9 dB at a bit rate of 10 Gbit/s.

1. Introduction

In recent years, optical wavelength division multiplexing (WDM) systems have been incorporated into commercial optical networks to satisfy data traffic demands. Furthermore, extensive studies aimed at enlarging network capacity and flexibility have been reported [1]-[3]. Wavelength converters will be key components in these WDM optical networks, and converters based on various principles and structures have been reported [4]-[7]. Among them, wavelength converters based on cross-phase-modulation (XPM) in a semiconductor optical amplifier (SOA) have several attractive features, such as a high extinction ratio, low chirp, and a waveform reshaping effect. Among XPM-SOA converters, those based on differential-phase-modulation (DPM), which utilizes XPM in a differential scheme, have been shown to be able to overcome the speed limitation imposed by the carrier lifetime in the SOA [8]. High-speed wavelength conversion of over 100 Gbit/s has been reported using DPM [9]. In this scheme, an optical filter is required in order to reject the input signal. In the case of wavelength tunable conversion, the response time of such filters may limit the system performance, and therefore filter-free operation is desirable [10]. In this paper, we report filter-free wavelength conversion at a bit rate of 10 Gbit/s using a newly developed Sagnac interferometer integrated with a parallel-amplifier structure (SIPAS). A power penalty as low as 0.9 dB was achieved in the fabricated SIPAS.

2. Structure and operating principle of the device

Figure 1 is a photograph of the fabricated SIPAS. The SIPAS is a Sagnac interferometer with a parallel-amplifier structure (PAS), which is a Mach-Zehnder interferometer (MZI) having polarization insensitive SOAs in each arm. The SOA has a pn-buried structure with a tensile-strained bulk InGaAsP active layer. The passive waveguides constructing the interferometers have a high-mesa structure. The SIPAS was fabricated monolithically by butt-coupling the high-mesa and buried waveguides [11]. The SOA length is 600 μm and total chip size is 4.5 mm × 1.5 mm.

The working principle of our device is shown in Fig. 2 An input CW light is divided into clockwise (CLW) and counterclockwise (CCW) traveling lights. Since the PAS is asymmetrically placed in the loop,
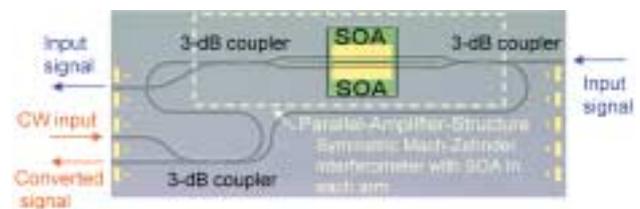

Fig. 1. Photograph of the SIPAS.

† NTT Photonics Laboratories
Atsugi-shi, 243-0198 Japan
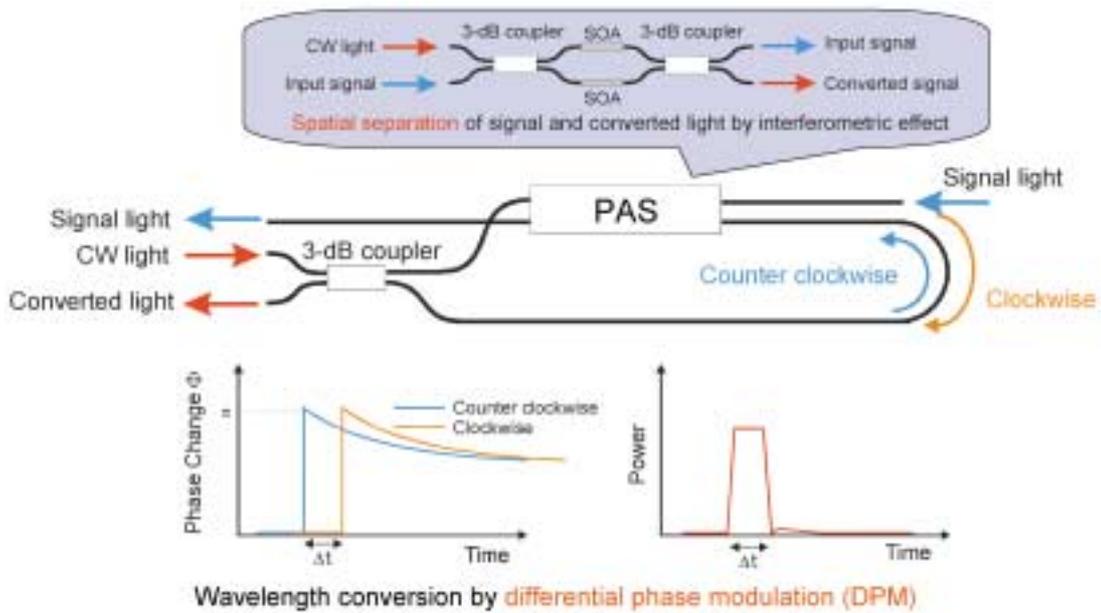E-mail: yshibata@aecl.ntt.co.jp

Fig. 2.　Working principle of SIPAS.

the CLW and CCW lights reach the SOAs at different times, which leads to different phase modulation between CLW and CCW lights when signal light is input into the SOAs. After traversing the loop, CLW and CCW lights are superimposed and transmitted to the output port due to DPM. We placed the PAS asymmetrically by 0.5 mm so that the switching window due to DPM becomes about 11 ps, which enables high-speed operation at over 40 Gbit/s. As the PAS is a symmetrical Mach-Zehnder interferometer, it can be set to the cross-state by injecting the same driving current into both SOAs. In the cross-state, the signal and CW lights are fed to different output ports when they are input from different input ports [12], so the signal light cannot enter the loop, resulting in filter-free wavelength conversion.

3. Design and fabrication

In order to build monolithically integrated devices like the SIPAS, it is necessary to fabricate a high-performance active region and low-loss passive region at the same time. To meet this demand, we utilized the pn-buried structure, which is popular in SOAs, for the active region, and a high-mesa structure [13], which has low propagation loss and is very effective for minimizing circuit size, for the passive region. To maximize the coupling efficiency between buried waveguides and high-mesa waveguides, the width of the buried waveguide should be between 1.2 and 1.5 μm because the width of the high-mesa waveguide is

between 2.0 and 2.5 μm. Considering the single-mode limitation, the core thickness of the buried waveguide should be between 0.1 and 0.3 μm.

Generally, the gain G (dB) of an SOA can be represented as:

$$G = 10 \log (\exp (\Gamma g L)),$$

where g is the gain coefficient, L the SOA length, and Γ the optical confinement factor in the active layer. The polarization-dependent gain difference ΔG (dB) can be represented by

$$\Delta G = G_{TE} - G_{TM}$$
$$\propto g_{TE} \Gamma_{TE} - g_{TM} \Gamma_{TM},$$

where G_{TE} and G_{TM} are the gains, g_{TE} and g_{TM} are
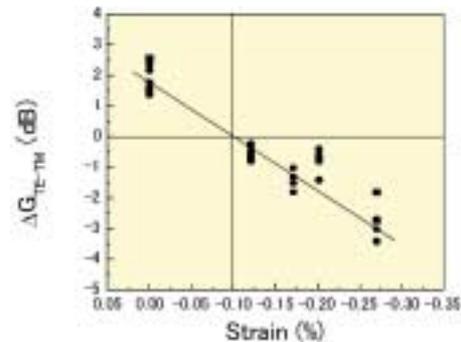

Fig. 3.　Difference in gain for TE and TM polarized lights as a function of strain when $\Gamma_{TE}/\Gamma_{TM} = 1.2$.
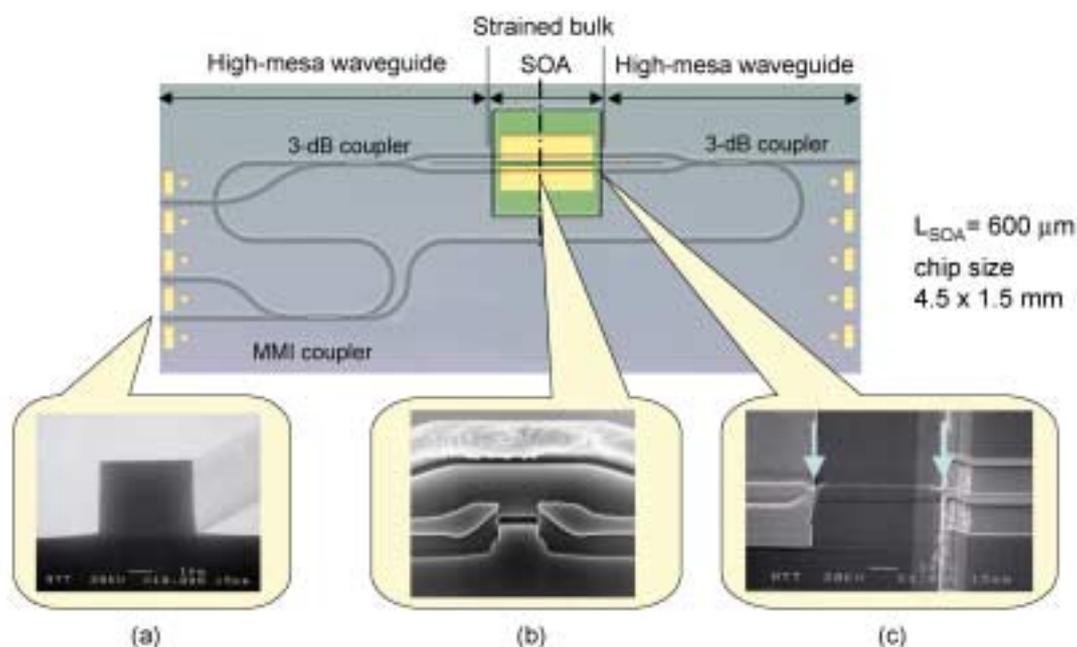
Fig. 4.   SEM photograph of the fabricated device.
(a) Cross-sectional view of the high-mesa passive waveguide. (b) Cross-sectional view
of the buried SOA. (c) Interface between high-mesa passive waveguide and SOA.

gain coefficients, and Γ_{TE} and Γ_{TM} are optical confinement factors for TE- and TM-polarized signal, respectively. When the cross section of an active layer is rectangular, as mentioned above, the optical confinement factor has polarization dependence, and Γ_{TE} becomes larger than Γ_{TM}. In order to realize a polarization-insensitive SOA ($\Delta G = 0$), the gain coefficient g should have polarization dependence and compensate for the polarization dependence of the optical confinement factor Γ. The polarization dependence of the gain coefficient g can be controlled by introducing a strain into the active layer. When the lattice constant of the active layer is smaller than that of the substrate, the active layer is tensilely strained in the plane parallel to the substrate surface. This introduces anisotropy in the gain coefficient g, and, as a result, the gain coefficient for TM-mode g_{TM} increases. Thus, the condition $g_{TE} \Gamma_{TE} = g_{TM} \Gamma_{TM}$ is achieved [14], [15]. Figure 3 shows the difference in gain for TE and TM polarized lights as a function of strain when $\Gamma_{TE}/\Gamma_{TM} = 1.2$. This figure shows the case when the chip gain is 10 dB per 300 μm. The slope is 1.8 dB per 0.1% change in strain. We can get a polarization-insensitive SOA by using a tensile strain of 0.1%. As the long-term reliability can be guaranteed at a strain of around 0.1%, we utilized the tensile-strained bulk layer as the active layer of the SOAs.

The fabrication process is briefly as follows: First,

the active layer of the SOA, which consists of a 0.2-μm-thick 0.1%-tensile-strained InGaAsP layer ($\lambda_g = 1.53$ μm) with a 0.1-μm-thick upper separate confinement heterostructure (SCH) layer ($\lambda_g = 1.2$ μm) was grown on an InP substrate. After that, the 0.5-μm-thick InGaAsP core ($\lambda_g = 1.05$ μm) and 1.0-μm-thick InP cladding layer were butt-jointed. Next, the SOA stripe was dry etched, and embedded by a p-n blocking layer and p-doped InP cladding layer. Then, the p-n blocking layer and p-doped InP cladding layer, which were grown over the passive region, were removed to reduce the propagation loss of the passive waveguide. Finally, high-mesa passive waveguides that compose the Sagnac and Mach-Zehnder
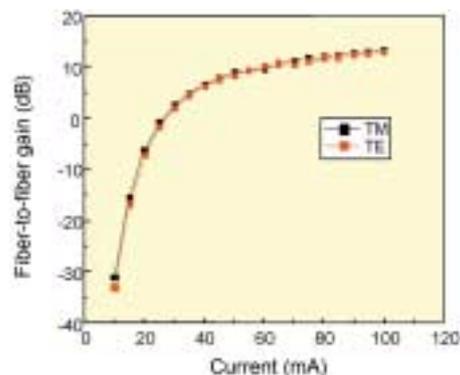

Fig. 5.   Gain-current characteristics of strained-bulk SOA.

interferometers were fabricated by Br_2-N_2 reactive beam etching [16]. The propagation loss of the high-mesa passive waveguide is about 5 dB/cm. The coupling loss between the SOA and passive regions is about 1 dB, including the active-to-passive coupling loss and the high-mesa-to-buried coupling loss.

Figure 4 shows an SEM photograph of the fabricated device. Figure 4(a) shows a cross-sectional view of the high-mesa passive waveguide. A smooth, almost vertical sidewall can be seen. The propagation loss of this high-mesa passive waveguide is about 5 dB/cm. The increase in loss due to the monolithic integration process is about 3 dB/cm. Figure 4(b) shows a cross-sectional view of the buried SOA. It shows that the p-n blocking layer was placed at the desired position. This is because the SOA fabrication process is the same as that for the conventional SOA, so the characteristics of the SOA are the same as those of a conventional one and are not degraded by the integration of passive waveguides. Figure 4(c) shows the interface between high-mesa passive waveguide and SOA.

Waveguides with completely different structures are well joined. The coupling loss between the SOA and passive regions is about 1 dB, including the active-to-passive and high-mesa-to-buried coupling losses.

4. Device characteristics

First, the basic characteristics of the SOA with a tensile-strained bulk active layer were investigated. Figure 5 shows the gain-current characteristics of an SOA with a passive waveguide. The lengths of the SOA active region and passive waveguide are 600 and 400 μm, respectively. Input signal wavelength was 1560 nm and input power was -10 dBm. Input light was coupled into the device using a polarization-maintaining lensed fiber, and output light was coupled using another lensed fiber. Fiber-to-fiber gain exceeded 13 dB and the polarization dependence of the gain was less than 1 dB. The influence of reflection at the interface between the buried SOA and passive high-mesa waveguide was not observed. This
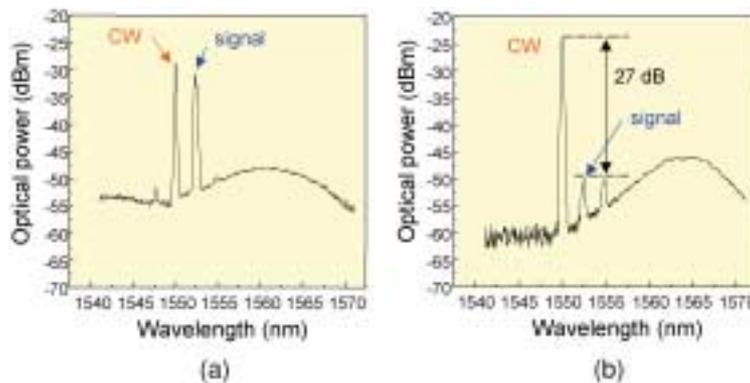

Fig. 6.   Spectrum from the output port when driving current was injected into (a) only SOA1 and (b) both SOAs.
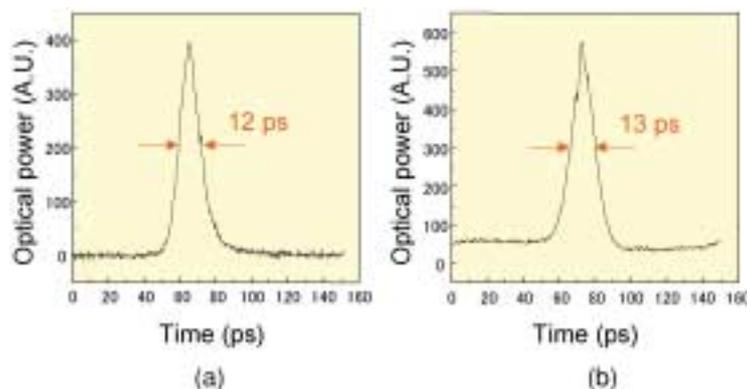

Fig. 7.   Optical waveforms of (a) input signal and (b) converted signal, respectively.
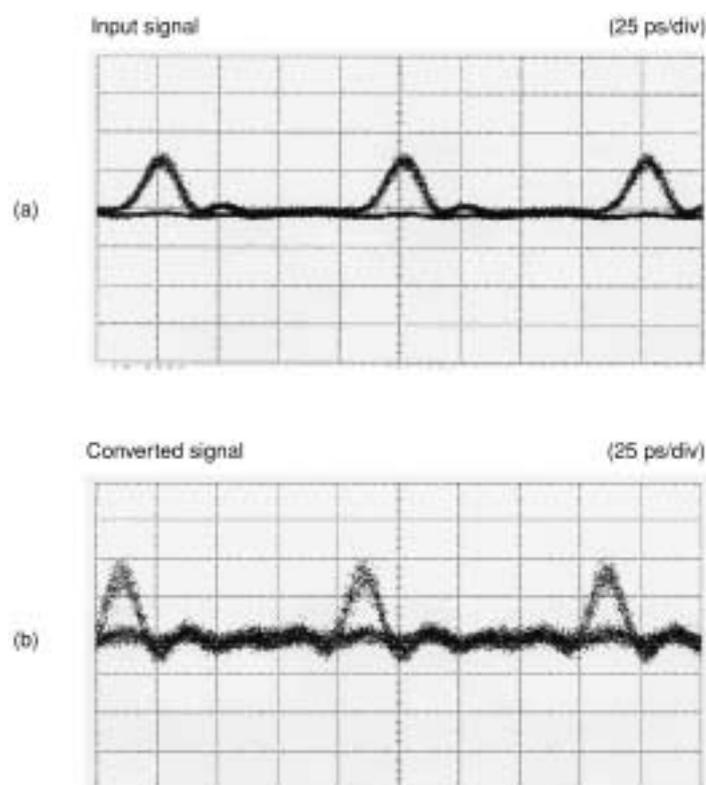
Fig. 8.   Eye diagrams of (a) input signal and (b) converted signal, respectively.

shows that these waveguides are joined quite well, not only physically but also optically.

Next, the filtering effect of the SIPAS was examined. A CW light and signal light were injected from the CW and signal input port, respectively. The wavelengths of the signal and CW lights were 1552.6 and 1550.0 nm, respectively. Input powers of the signal and CW lights were both 5 dBm. Figure 6 shows the spectrum from the output port. Figure 6(a) shows the spectrum from the output port when driving current of 217 mA was injected into only SOA1. In this case, SOA2 was absorptive because driving current was not injected, and as a result, interference could not occur in the PAS. As a result, the input signal penetrated into the Sagnac loop and the input signal and converted lights were output equally, as shown in Fig. 6(a). On the other hand, when drive currents of 212 and 217 mA were injected into SOA1 and SOA2, respectively, interference occurred in the PAS. As the PAS has a symmetric structure, almost the same injection currents set the PAS in the cross-state. This enabled spatial separation of input and converted signals, and the input signal light could not enter the Sagnac loop. As a result, only the converted signal was output, as shown in Fig. 6(b). The suppression

ratio was as large as 27 dB, as shown in the figure, which is large enough for filter-free operation. This is the most important feature of the SIPAS.

The operation of the SIPAS is due to DPM between the CLW and CCW lights. Then we next examined the DPM characteristics by observing the waveforms of the input and wavelength-converted signal with a streak camera. The operating conditions were the same as those in the filter-free condition described above. Figures 7(a) and (b) show the waveforms of the input and converted signals, respectively. The input pulse width was 12 ps and the repetition rate was 1 GHz. We placed the PAS asymmetrically by 0.5 mm so that the propagation delay time between the CLW and CCW light was about 11 ps. The output pulse width was 13 ps, which is very close to the expected value of 11 ps. This is evidence of DPM operation.

These experimental results show that fast wavelength conversion due to the DPM is achieved in the filter-free condition using the SIPAS. Finally, we investigated the dynamic characteristics of filter-free wavelength conversion. Figure 8 shows the eye diagrams of the input and wavelength-converted signals at a bit rate of 10 Gbit/s. The average powers of the
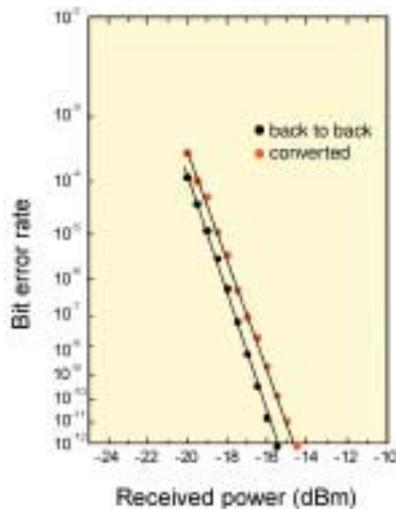
Fig. 9.   Bit-error-rate characteristics at a bit rate of 10 Gbit/s.

input signal and CW lights were 7.9 and 13.0 dBm, respectively. Clear eye opening was obtained. The corresponding bit-error-rate characteristics are shown in Fig. 9. The power penalty, which is defined as the sensitivity degradation at a bit-error-rate of 10^{-12}, was as low as 0.9 dB. The origin of this power penalty is thought to be the accumulation of amplified spontaneous emission from the SOAs.

In this paper, we have presented only experimental results at a bit rate of 10 Gbit/s. However, to date, we have confirmed filter-free operation at up to 40 Gbit/s. In a SIPAS, the width of the output window (output pulse width) and the repetition rate can be independently designed. This enables the SIPAS to be used not only in wavelength conversion, but also in all-optical demultiplexing. For example, when the output window is 11 ps and the repetition rate is 10 GHz, SIPAS can be used for demultiplexing from 80 to 10 Gbit/s. Additionally, due to the filter-free feature of the SIPAS, wavelength conversion in which the output wavelength changes dynamically is possible. This enables optical packet routing where packet-by-packet wavelength routing is performed using wavelength conversion. SIPAS is a device having many unique features, and we are now making further progress, including studying its application to all-optical 3R.

5. Summary

SIPAS is a wavelength conversion device having a new optical circuit structure. It is fabricated using semiconductor monolithic integration technology. It consists of a Sagnac interferometer with a parallel-amplifier structure, which is a Mach-Zehnder interferometer having polarization-insensitive SOAs in each arm. The most important feature of the SIPAS is filter-free operation.

We have developed a monolithically integrated SIPAS by using high-mesa waveguides and pn-buried SOAs with a tensile-strained active layer. Using the fabricated SIPAS, we have achieved filter-free wavelength conversion with an output window of 13 ps due to differential-phase-modulation. The power penalty was as low as 0.9 dB at a bit-rate of 10 Gbit/s.

References

[1] K. Habara, Y. Yamada, A. Misawa, K. Sasayama, M. Tsukada, T. Matsunaga, and K. Yukimatsu, "Demonstration of frequency routing type photonic ATM switch prototype," ECOC'96, Oslo, Norway, ThC. 3.4, Vol. 5, pp. 41-42, Sep. 1996.

[2] M. Koga, Y. Hamazumi, A. Watanabe, S. Okamoto, H. Obara, K. Sato, M. Okuno, and S. Suzuki, "Design and performance of an optical path cross-connect system based on wavelength path connect," J. Lightwave Technol., Vol. 14, No. 6, pp. 1106-1119, 1996.

[3] C. A. Brackett, A. S. Acampora, J. Sweitzer, G. Tangonan, M. T. Smith, W. Lennon, K. Wang, and R. H. Hobbs, "A scalable multiwavelength multihop optical network: A proposal for research on all-optical networks," J. Lightwave Technol., Vol. 11, No. 5, pp. 736-753, 1993.

[4] T. Durhuus, C. Joergensen, B. Mikkelsen, R. J. S. Pedersen, and K. E. Stubkjaer, "All-optical wavelength conversion by SOA's in Mach-Zehnder configuration," IEEE Photon. Technol. Lett., Vol. 6, No. 1, pp. 53-55, 1994.

[5] T. Durhuus, B. Mikkelsen, C. Joergensen, S. L. Danielsen, and K. E. Stubkjaer, "All-optical wavelength conversion by semiconductor optical amplifiers," J. Lightwave Technol., Vol. 14, No. 6, pp. 942-954, 1996.

[6] R. Ludwig, and G. Raybon, "BER measurements of frequency converted signals using four-wave mixing in a semiconductor laser amplifier at 1, 2.5, and 10 Gbit/s," Electron. Lett., Vol. 30, No. 4, pp. 338-339, 1994.

[7] S. J. B. Yoo, "Wavelength conversion technologies for WDM network applications," J. Lightwave Technol., Vol. 14, No. 6, pp. 955-966, 1996.

[8] B. Mikkelsen, K. S. Jepsen, M. Vaa, H. N. Poulsen, K. E. Stubkjaer, R. Hess, M. Duelk, W. Vogt, E. Gamper, E. Gini, P. A. Besse, H. Melchior, S. Bouchoule, and F. Devaux, "All-optical wavelength converter scheme for high speed RZ signal formats," Electron. Lett., Vol. 33, No. 25, pp. 2137-2139, 1997.

[9] S. Nakamura, Y. Ueno, and K. Tajima, "168-Gb/s all-optical wavelength conversion with a symmetric-Mach-Zehnder-type switch," IEEE Photon. Technol. Lett., Vol. 13, No. 10, pp. 1091-1093, 2001.

[10] J. Leuthold, J. Eckner, P. A. Besse, G. Guekos, and H. Melchhior, "Dual-order mode (DOMO) all-optical space switch for bi-directional operation," OFC'96, San Jose, California, U.S.A., Paper ThQ1, pp. 271-272, Feb. 1996.

[11] H. Ishii, M. Kohtoku, Y. Shibata, S. Oku, Y. Kadota, Y. Yoshikuni, H. Sanjo, Y. Kondo, and K. Kishi, "Zero Insertion Loss Operations in Monolithically Integrated WDM Channel Selectors," IEEE Photon. Technol. Lett., Vol. 11, No. 2, pp. 242-244, 1999.

[12] Y. Shibata, N. Kikuchi, S. Oku, T. Ito, H. Okamoto, Y. Kawaguchi, Y. Suzuki, and Y. Kondo, "Monolithically Integrated Parallel-Amplifier Structure for Filter-free Wavelength Conversion," IPRM'01, Nara, Japan, FB1-5, pp. 587-590, May 2001.

[13] N. Yoshimoto, Y. Shibata, S. Oku, S. Kondo, Y. Noguchi, K. Wakita, and M. Naganuma, "Fully Polarization Independent Mach-Zehnder Optical Switch using a Lattice Matched InGaAlAs/InAlAs MQW and High-mesa Waveguide Structures," Electron. Lett., Vol. 32, No. 15, pp. 1368-1369, 1996.

[14] J. Y. Emery, T. Ducellier, M. Bachmann, P. Doussière, F. Pommereau, R. Ngo, F. Gaborit, L. Goldstein, G. Laube, and J. Barrau, "High performance 1.55 μm polarization-insensitive semiconductor optical amplifier based on low-tensile-strained bulk GaInAsP," Electron. Lett., Vol. 33, pp. 1083-1084, 1997.

[15] T. Kakitsuka, Y. Shibata, M. Itoh, Y. Tohmori, and Y. Yoshikuni, "Theoretical analysis of polarization sensitivity of strained bulk SOAs," SPIE Optoelectronics 2001, San Jose, U.S.A., 4283-48, Jan. 2001.

[16] S. Oku, Y. Shibata, and K. Ochiai, "Controlled beam dry etching of InP by using Br_2-N_2 gas," J. Electron. Mater., Vol. 25, No. 4, pp. 585-591, 1996.

Yasuo Shibata
Senior Research Engineer, Photonic Device Laboratory, NTT Photonics Laboratories.
He received the B.E. and M.E. degrees in electrical engineering from Keio University, Kanagawa, Japan in 1985 and 1987, respectively. In 1987, he joined NTT Optoelectronics Laboratories, where he has been engaged in research on optical switches and optical filters. He is currently with NTT Photonics Laboratories, engaged in research on SOA and wavelength-conversion devices. Mr. Shibata is a member of the Japan Society of Applied Physics, and the Institute of Electronics, Information and Communication Engineers (IEICE).

Yuichi Tohmori
Senior Research Engineer, Supervisor, Photonic Device Laboratory, NTT Photonics Laboratories.
He received the B.E., M.E., and Ph.D. degrees from the Tokyo Institute of Technology, Tokyo, Japan, in 1981, 1983, and 1986, respectively. In 1986, he joined the NTT Optoelectronics Laboratories, Nippon Telegraph and Telephone Corporation (NTT), where he engaged in the research on the development of narrow linewidth lasers and wavelength tunable DBR lasers, spot-size converter integrated lasers, and the integrated devices using lasers and semiconductor optical amplifiers.
Dr. Tohmori is a member of IEICE, JSAP, OSA, and a senior member of IEEE/LEOS.

Satoshi Oku
Senior Research Engineer, Photonic Device Laboratory, NTT Photonics Laboratories.
He received the B. E., M. E., and Ph. D. degrees from Kyoto University, Kyoto Japan in 1977, 1979 and 2000, respectively.
He joined Musashino Electrical Laboratories, NTT Corporation, Tokyo, Japan, where he was engaged in research on ultra-low loss optical fiber materials and integrated optical materials. Since 1987, he has been engaged in research on integrated semiconductor optical devices at NTT Photonics Laboratories, Kanagawa, Japan. Dr. Oku is a member of the Japan Society of Applied Physics and the Institute of Electronics, Information and Communication Engineers (IEICE) of Japan.

Toshio Ito
Senior Research Engineer, Photonics Integration Project, NTT Photonics Laboratories.
He received the B.E., M.E., and Ph. D degrees from Keio University, Kanagawa, Japan, in 1986, 1988, and 2003, respectively. In 1988, he joined the Musashino Electrical Communications Laboratories, where he engaged in research on parallel processing systems and communication switching systems. Since 1993, he has been engaged in research on the InGaAlAs/InAlAs multi-quantum well optical switches, InGaAsP semiconductor optical amplifiers, and wavelength converters at NTT Photonics Laboratories. Dr. Ito is a member of the IEICE, JSAP, and OSA.